

FIG 1. Global supercoiling did not vary under treatment of *S. pneumoniae* R6 (pLS1) with levofloxacin. (A) Viability. (B) Topoisomer distribution of pLS1. Exponentially growing cultures in AGCH at $OD_{620nm} = 0.4$ were treated with the indicated LVX concentrations. Values of a typical experiment are indicated. Samples were taken before the addition of the drug (time 0 min), and, at the indicated times, plasmid DNA was isolated and subjected to two-dimensional agarose electrophoresis run in the presence of 1 and 2 $\mu\text{g/ml}$ chloroquine in the first and second dimensions, respectively. Supercoiling density (σ) values are indicated. A black arrowhead indicates the topoisomer that migrated with $\Delta Lk = 0$ in the second dimension that has a $\Delta W_r = -14$. An empty arrowhead indicates the more abundant topoisomer.

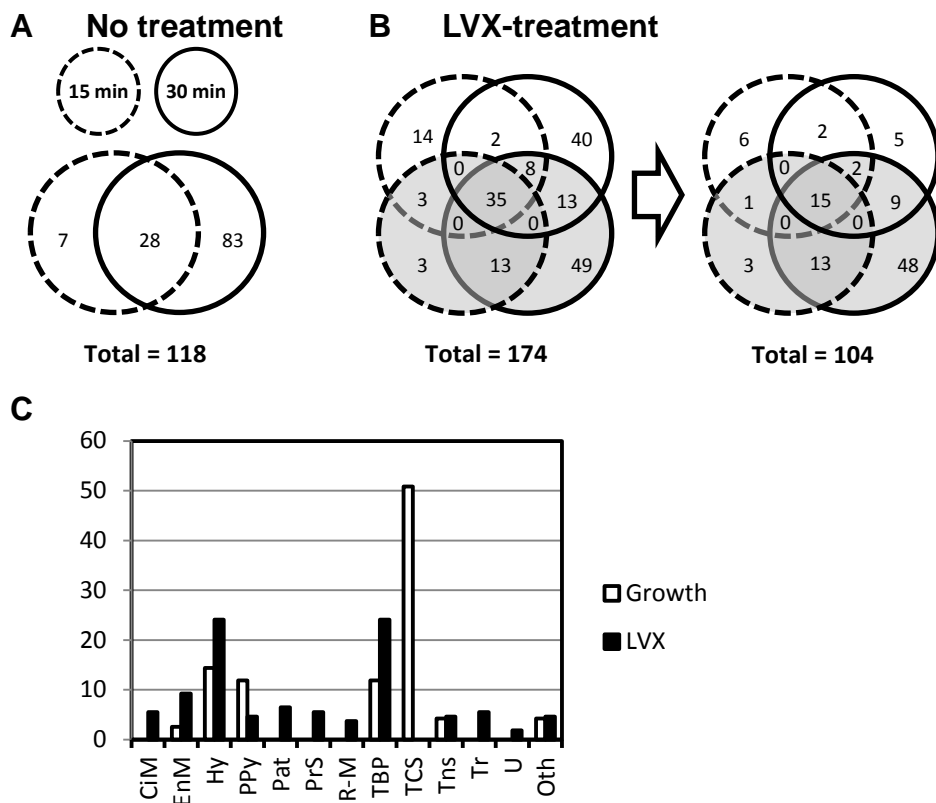


FIG 2. Gene expression analysis in the three conditions assayed. (A and B) Responsive genes represented in Venn diagrams with 3 circles, each one corresponding to one time interval in each condition, showing the differentially expressed genes in microarrays. (B) All genes (left diagram), or only those genes that differed from those present in the No-LVX sample (right diagram), are indicated. A complete list of these genes can be found in Table S1. (C) Classification of responsive genes by functional classes: Pat, pathogenesis; CiM, central intermediary metabolism; EnM, energy metabolism; Hy, hypothetical proteins; PPy, Purines, pyrimidines, nucleosides, and nucleotides; PrS, protein synthesis; R-M, restriction-modification; TBP, transport and binding proteins; TCS, two-component systems; Tns, transposon functions; Tr, transcription; U, unclassified; Oth, other (classes with a representation lower than 2%).

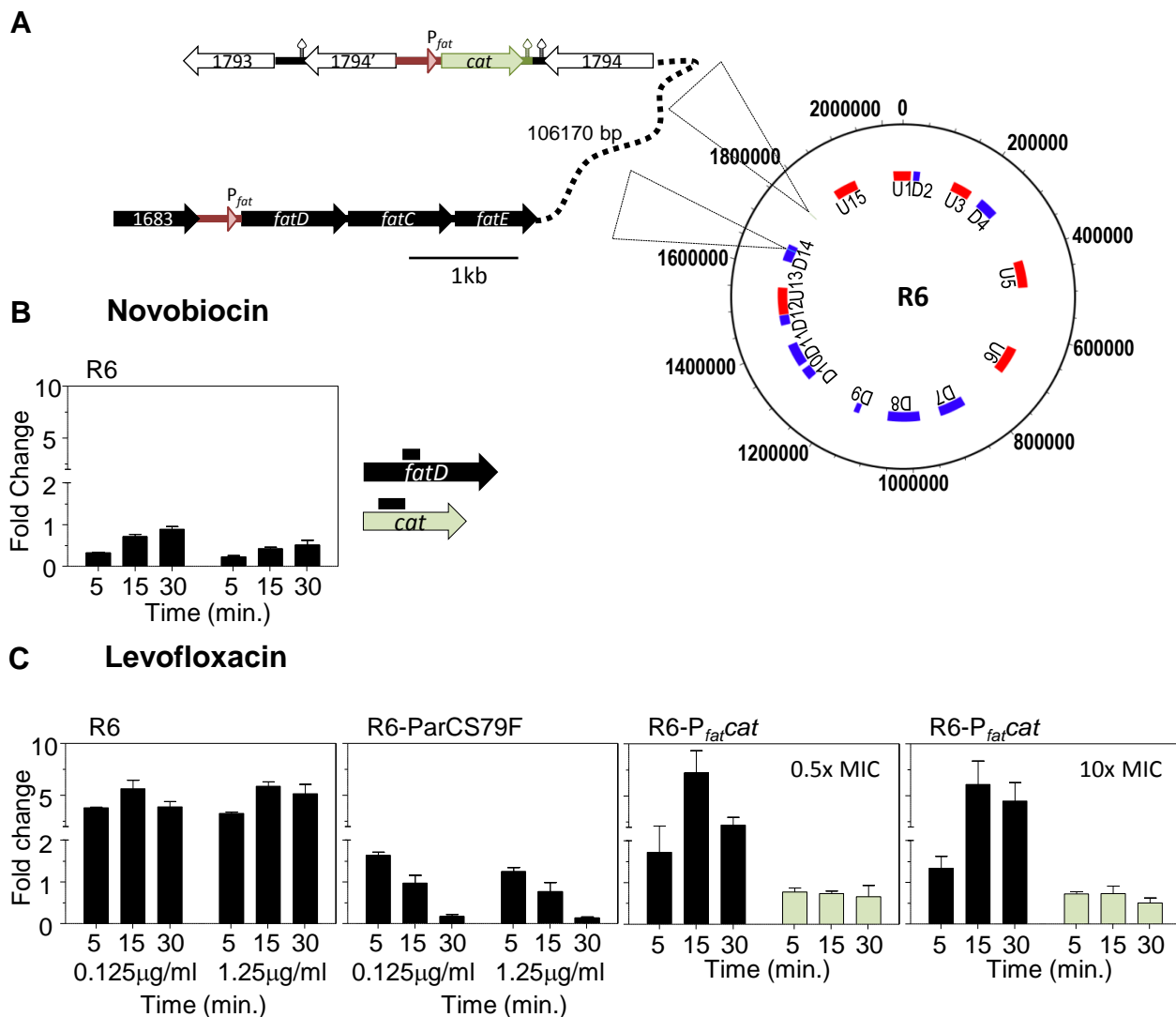


FIG 3. Transcription of *fatD* depended on the inhibition of topoisomerase IV by LVX. (A) Genetic structure of strain R6-*P_{fat}cat* showing the chromosomal location of *P_{fat}fatDCEB* and *P_{fat}cat*. Topology-reacting gene clusters detected after DNA relaxation with novobiocin are indicated: U1-15, up-regulated domains; D1-14, down-regulated domains. (B) Transcriptional response after novobiocin treatment measured by qRT-PCR on exponentially growing cultures of strain R6. (C) Transcriptional response of R6, of a LVX-resistant derivative (R6-ParCS79F), and of the R6-*P_{fat}cat* strain. Cultures were grown in AGCH to $OD_{620nm}=0.4$, treated with LVX at 0.125 μg/ml LVX (0.5× MIC of R6 and R6-*P_{fat}cat*; 0.05× MIC of R6-ParCS79F) and at 2.5 μg/ml LVX (10× MIC of R6 and R6-*P_{fat}cat*; 0.5× MIC of R6-ParCS79F). Total RNA was isolated; cDNA was synthesized and subjected to qRT-PCR. Data were normalized to time 0 min. Transcription represented the mean of qRT-PCR values of three independent replicates ± SEM.

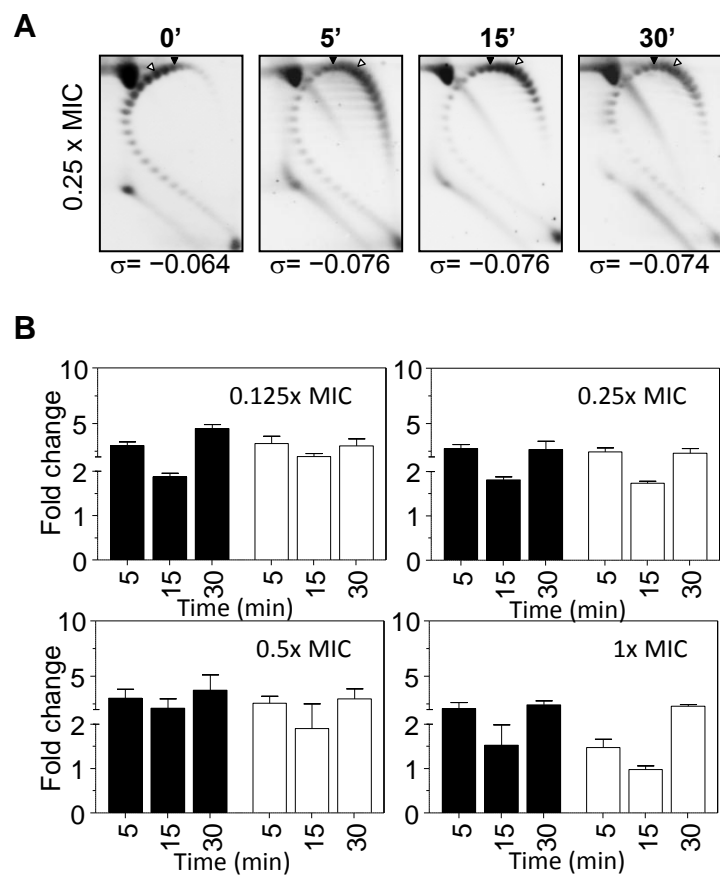


FIG 4. Transcription of *fatD* depended on the general supercoiling level. Cultures were grown as in Fig. 3 and treated with N-methyl-seconeolitsine at the indicated concentrations. (A) Plasmid DNA was isolated at the indicated times and subjected to two-dimensional agarose electrophoresis run in the presence of 5 and 15 $\mu\text{g/ml}$ chloroquine in the first and second dimensions, respectively. Supercoiling density (σ) values are indicated. A black arrowhead indicates the topoisomer that migrated with $\Delta\text{Lk} = 0$ in the second dimension that has a $\Delta\text{Wr} = -30$ (53). An empty arrowhead indicates the more abundant topoisomer. (B) Total RNA was isolated; cDNA was synthesized and subjected to qRT-PCR, *fatD* and *fatC* values were normalized to time 0 min. Transcription represented the mean of qRT-PCR values of three independent replicates \pm SEM.

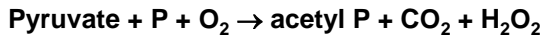
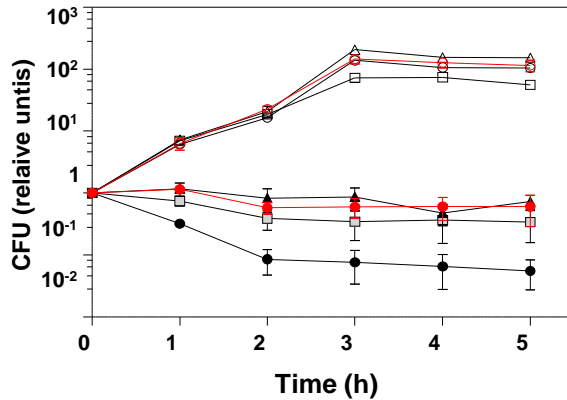
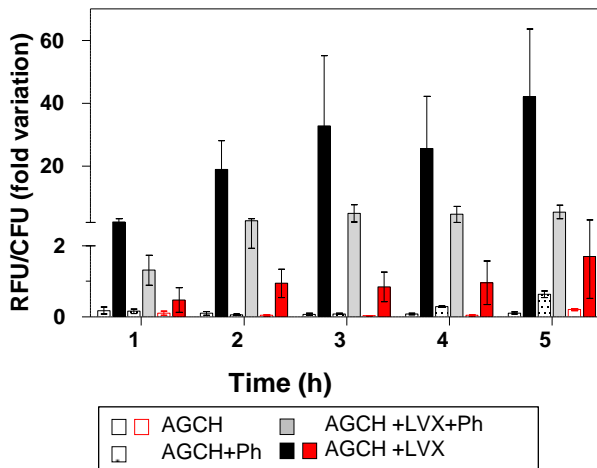
A**SpxB reaction:****Fenton Reaction:****B****C**

FIG 5. LVX lethality is related to the level of intracellular iron. (A) Enzymatic reaction of SpxB that renders H_2O_2 , a substrate of the Fenton reaction. (B) Viability of *S. pneumoniae* R6 (black symbols) or R6 Δ spxB (red symbols) either in AGCH, in AGCH plus the iron chelator *o*-phenantroline (AGCH+ Ph), in AGCH deficient in SO_4Fe (AGCH*). Cultures grown as indicated in Fig. 3 in the diverse media were treated, when indicated, with LVX at concentrations equivalent to $2.5\times$ MIC. (C) Accumulation of reactive oxygen species. Results are the mean \pm SEM of three independent replicates. RFU, relative fluorescence units, values were made relative to 0 min and divided by the number of viable cells.

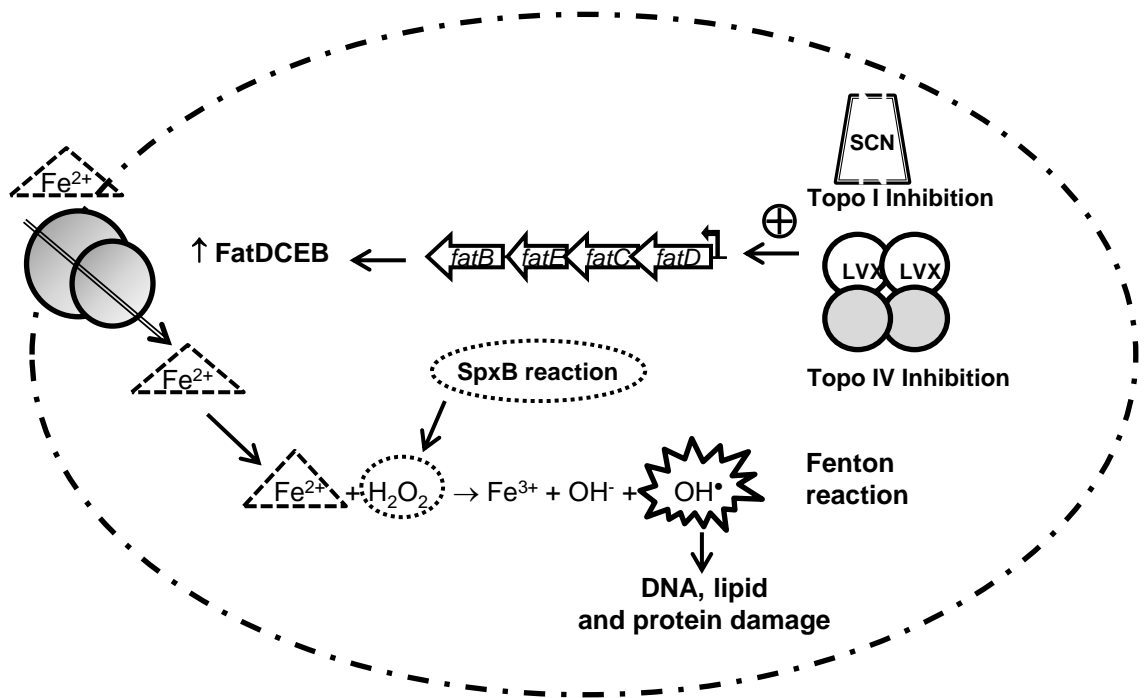


FIG 6. Oxidative damage cell death pathway. The inhibition of topo IV by levofloxacin (LVX) or of topoisomerase I by N-methyl-seconeolitsine (SCN) would cause a local increase in supercoiling resulting in the up-regulation of the *fatDCEB* operon. The consequent increase in this iron transporter caused an increase of intracellular ferrous iron (Fe^{2+}). This compound and hydrogen peroxide (produced by the activity of the SpxB enzyme) are the substrates of the Fenton reaction. The Fenton reaction renders hydroxyl radicals, which oxidatively damage DNA, proteins and lipids.